A sustainable, eugenol-derived epoxy resin with high biobased content, modulus, hardness and low flammability: Synthesis, curing kinetics and structure-property relationship

Jintao Wan[a], Bin Gan[a], Cheng Li[a,b], Jon Molina-Aldareguia[a], Ehsan Naderi Kalali[a], Xin Wang[a], and De-Yi Wang*[a]

a. IMDEA Materials Institute, C/Eric Kandel, 2, 28906 Getafe, Madrid, Spain

b. State Key Laboratory of Chemical Engineering, College of Chemical and Biological Engineering, Zhejiang University, Hangzhou 310027, China

*Corresponding author

E-mail: deyi.wang@imdea.org Phone: +34 91 787 1888. Fax: + 34 91 550 3047

Abstract: To develop functional sustainable epoxy resins, we report a novel epoxy resin (DEU-EP) with high net biobased content (70.2 wt%) derived from renewable eugenol. We comparatively study DEU-EP with a commercial bisphenol A epoxy resin (DGEBA) in the presence of a most representative aromatic diamine curing agent, 4,4'-diaminodiphenyl methane (DDM). Differential scanning calorimetry reveals that DEU-EP can be sufficiently cured by DDM at a slower rate than DGEBA. By applying an autocatalytic reaction model, we adequately simulate the curing rate of DEU-EP/DDM, and reveal its detailed kinetic mechanisms from model-free isoconversional analysis. Dynamic mechanical analysis shows that DEU-EP/DDM takes higher storage modulus up to ~97 ^{o}C than DGEBA/DDM with the glass temperature of 114 ^{o}C. Nanoindentation and thermogravimetric analysis demonstrate that compared with DGEBA/DDM, DEU-EP/DDM exhibits a 20%, 6.7% and 111% increase in Young's modulus, hardness and char yield, respectively. Microscale combustion calorimetry data show that DEU-EP/DDM expresses 55% and 38% lower heat release rate and total heat release than DGEBA/DDM, respectively. Macroscopically, the horizontal burning test approves DEU-EP/DDM can self-extinguish in a short time. Our results demonstrate that the eugenol building blocks and their arrangement greatly affect the cure behaviors of DEU-EP/DDM, and contribute significantly to its enhanced mechanical properties, high-temperature charring ability and chain motions at glass state, as well as the reduced flammability. To summarize, DEU-EP exhibits a high promise as a new sustainable epoxy monomer for fabricating high biobased content, high rigid and low flammable epoxy materials.

Keywords: Biobased epoxy resin; curing reaction kinetics; isoconversional analysis; mechanical and thermal properties; flammability.

1. Introduction

Epoxy resins find wide applications in protective coatings, insulating and embedding materials, structural adhesives, composites, construction materials and so forth starting from 1947. These applications are mainly due to attractive properties of epoxy resins including excellent chemical resistance, superior mechanical properties, amenability to a variety of formulating techniques, and highly versatile applicability. Before cure, epoxy monomers or oligomers have more than one epoxy groups; after cure, they become a highly cross-linked macromolecule with the help of a suitable curing agent (co-cure) or a catalysis (self-cure). Sometimes inorganic fillers, fibers, reactive diluent, pigments and flame retardant are introduced into epoxy curing systems to increase thermal, mechanical and electric properties, processablity, wetting ability, flame retardancy and so on to meet more specific and/or demanding applications [1, 2]. Now, great majority of epoxy resins (approximately >90% market share) are synthesized from the bisphenol A (BPA) and epichlorohydrin via an O-glycidylation reaction. This O-glycidylation may follow the two general mechanisms: [3] (1) the direct nucleophilic substitution (SN_2) of phenolate ion (ArO^-) by epichlorohydrin, with the cleavage of C-Cl bond; (2) ArO^- causes the opening of epichlorohydrin ring, followed by a ring closing reaction in the help a strong base. Depending on the molar ratio of bisphenol A to epichlorohydrin, synthetic conditions and separation techniques, molecular weights of DGEBAs may range from 340 Da for pure bisphenol A diglycidyl ether to several thousand for glycidyl end-capped bisphenol A-co-epichlorohydrin oligomers. At room temperature, DGEBAs may be a crystal, liquid or amorphous glassy solid dependent on their molecular weight and purify.

Besides the bisphenol A-based epoxy resins, theoretically these compounds bearing at least two non-aromatic double bonds can be converted to the corresponding epoxy resins through epoxidation reaction of these double bonds. Peroxyacids are widely used to convert the double bonds of to the corresponding epoxy groups. In particular, peroxyacetic acid and peroxyformic acid formed in situ from acetic/formic acids and high-concertation hydrogen peroxide solution are widely used to epoxidize the precursors the corresponding epoxy resins under optimal kinetic conditions [4, 5]. These processes play an extremely important role for the industrial production of epoxy resins from corresponding double-bond compounds, due to the relatively low cost and negative environment impact. In contrast, meta-chloroperoxybenzoic acid (mCPBA) is able to more directly convert the double bonds of a large number of Alkenes to the corresponding epoxy compound with high selectivity in methylene chloride under wild conditions, which are widely used in lab-scale synthesis of epoxy compounds from their double bond parent compounds.

As main materials for producing DGEBAs, BPA is synthesized from unrenewable acetone and phenol. In particular, phenol is classified as the high toxic materials and dominant commercial route to phenol is based on the Hock oxidation of benzene-derived cumene. About 20% of global benzene production was used to manufacture to bisphenol

A. Although an alternative way to synthesize from glucose has been reported [6], but the industrial scale-up of this biobased process is still far from being achieved. On the other hand, epichlorohydrin is highly toxic and mainly produced from allyl chloride, and using renewable and nontoxic glycerol to produce epichlorohydrin is another sustainable alternative [7, 8], showing a great commercial importance in the further. BPA is widely used to manufacture epoxy resins and certain plastics such as polycarbonate for making milk bottles. However, due to its identified and suspected hazards to fetuses, infants and young children, many countries have banned BPA remaining in milk bottles. Therefore, to reduce the toxic risks during the product and use of DGEBAs, there is a strong desire to replace BPA to synthesize epoxy resins. In addition, DGEBAs are inherently high in flammability, and traditional methods to improve this property are mainly to introduce halogen element/compounds into the of the epoxy resin systems. However, halogenated flame retardant epoxy resin systems are not welcomed especially in EU. For sustainable development, it is of great interest to make use of renewable biomasses to produce greener low flammable epoxy resins with enhanced properties.

With increasing scarcity of fossil resources and greenhouse gas effect, developing the environment friendly epoxy systems (including biobased epoxy curing agents) based on renewable biomasses becomes most a promising solution and attracts a lot of attention [9, 10]. Among a large variety of biomasses, vegetable oils are most sufficiently studied starting materials to synthesize epoxy resins (epoxied vegetable oils). Combination of epoxied vegetable oils and vegetable oil-based curing agents results in the total biobased epoxy systems taking the advantage of high biomass contents [11]. Moreover, Mija et al. [12] found that a suitable acid anhydride with a suitable catalysis under optimized curing condition was found to be able to endow epoxidized linseed oils with better properties. Webster et al. [13] reported epoxidized sucrose esters of fatty acids used as the epoxy monomer, and found that sucrose core can markedly improve mechanical and thermal properties of their 4-methyl hexahydrophthalic anhydride (MHHPA) cured epoxy product due to the very high epoxy functionalities and well-defined molecular structures. As an alternative, Huang, et al. [14], reported the epoxy resins based on the tung oil fatty acid-derived C_{21} diacid and C_{22} triacid showing better overall properties than epoxidized soybean oil (ESO). Interestingly, beyond traditional epoxy chemistry, another tung oil fatty acid-based epoxy monomer with synergistic curing characteristics was reported in 2014 [15]. Although this epoxy monomer contains only one epoxy group, it bears conjunction double bonds, so that it can react with specific anhydrides and bismaleimide through Diels–Alder and epoxy/anhydride ring-opening reactions to form the cross-linked thermosetting network.

On the other hand, epoxy resins derived from other more rigid biobased aromatic and other ring compounds with improved properties received a considerable interest in the recent years [9]. For example, in 2014 Palmese et al. [16] reported a furan-based epoxy resin and they found that this epoxy resin showed higher glass temperature and modulus that phenyl-based epoxy

resins of similar molecular structure. Petrović et al. [17] reported an epoxy systems based on water soluble isosorbide-based epoxy resin and isosorbide-based aliphatic amine curing agent. In 2015 Gross and coworkers reported diphenolic acid (DPA) based epoxy resins with controlled properties (viscosity, glass temperature and modulus) [18].

As far as eugenol (4-allyl-2-methoxyphenol) is concerned, it is an interesting naturally occurring, renewable phenol compound extracted from plant and some specific lignin [19]. For example, eugenol comprises approximately 70-90% of clove oil from eugenia caryophyllata and occurs widely as a component of essential oils [20] with relatively low cost (ca. \$5 kg^{-1}) [21]. These merits make eugenol economically feasible to synthesize biobased monomers or polymers. In particular, eugenol (LD50 Oral - rat - > 2000 mg/kg) is far less toxic than phenol (LD50 Oral - rat - 317 mg/kg) that is one of two starting materials for synthesizing bisphenol A. Structurally, eugenol bears a terminal olefin group and a hydroxyl group that provides the ability for polymerization and chemical modification, and moreover its aliphatic chain, methoxyl group, aromatic ring are expected have a great impact on the properties of polymers derived from eugenol [22]. To the best of our knowledge, however, so far only two kinds of eugenol-based epoxy resins have been reported. Kireev et al. [23, 24] reported the synthesis and structural characterization of epoxy resins derived from eugenol and hexachlorocyclotriphosphazene with a very high molecular weight, but did not address their cure and ultimate properties likely due to limitation of the processing ability. Another publication [25] reported a liquid eugenol-based epoxy resin (Eu-Ep) with two epoxy groups attached to one eugenol moieties, high theoretical epoxy value of 0.846 mol/100g and the biobased content of 62.7% (the inherent weight percentage from eugenol). Eu-Ep was synthesized via three steps (a protection step involved). Eu-EP could be well cured with commercial hexahydrophthalic anhydride in the presence of a 2-ethyl-4-methylimidazole catalyst, reaching the glass temperature of 114 ^{o}C.

From the primary results above, we notice that the biobased content of the eugenol-based epoxy resins still need further enhancing to make better use of eugenol. Moreover, the properties of the eugenol-based epoxy resins still need further improving especially mechanical properties and flammability. Especially, reducing flammability of DGEBAs based epoxy materials is an important topic in epoxy technology development. In addition, the laboratory synthesis and purification methods of eugenol-based epoxy resins still need improving to reduce the preparation steps and to facilitate the separation process. On the other hand, curing agents have a profound influence on curing reaction and properties of cured epoxy resin systems. The most important and widely used curing agents for epoxy resins belong to polyfunctional amine compounds (e.g., polyethylene polyamine and aromatic and alicyclic diamines). They, unlike anhydride curing agents (high temperature and catalyst are necessary), can be used alone without a catalyst to well cure epoxy systems in a suitable temperature range, even at room temperature (aliphatic amine curing agents). Amine curing agents account for the largest share of epoxy applications. Amine cured epoxy resins, especially cured with aromatic diamine curing agents, shows much better mechanical, chemical and solvent resistance than anhydride-cured

epoxy resins, so that they are wildly used in protective coatings. Therefore, a systematic study of cure behaviour and properties of eugenol-based epoxy resins in the presence of a most reprehensive amine curing agent will be much revealing and of practical importance. To our knowledge, however, there is still lack of systematic study on this area to date.

Here we report a novel eugenol-based epoxy resin (DEU-EP) prepared by a facile biobased route. As shown in Scheme 1, DEU-EP is synthesized by bridging two eugenol molecules together via a *p*-xylene linkage, followed by epoxidation of the two inherent allyl double bonds under a mild condition. Compared to previous reported eugenol-based epoxy resin (Eu-Ep) [25], DEU-EP's synthesis steps are reduced to two, its purification is simplified to avoid the column chromatography, and moreover DEU-EP has increased biobased content (62.7% vs. 70.2%). More interestingly, a**s** another starting material of DEU-EP, α,α'-dichloro-p-xylene, shows the great potential to be produced via a biobased route. α,α'-dichloro-p-xylene are produced from catalytic chlorination of p-xylene under light irritation, whereas p-xylene has been shown to be able to produce from cellulose-derived furans [26-28] and bio-isobutanol via biobased routes. In 2013 Gevo, Inc. has established a demonstration-scale p-xylene with bio-isobutanol as the starting material plant in Texas, USA [29]. In this sense, the starting materials of DEU-EP have the full potential to be produced via biobased routes, which will lead to even higher biobased content of DEU-EP, thus enabling DEU-EP more interesting and potentially sustainable. We will use a most widely used and representative aromatic diamine curing agent (4,4'-methylenedianiline (DDM)) to cure DEU-EP and compared DEU-EP with DGEBA of similar molecular weight (Scheme 2). We will elaborate on how the eugenol building blocks and their arrangement affect the curing behaviors and properties of DEU-EP different from a DGEBA. Our results will show that DDM-cured DEU-EP not only has enhanced mechanical properties (modulus and hardness) but also greatly reduced flammability.

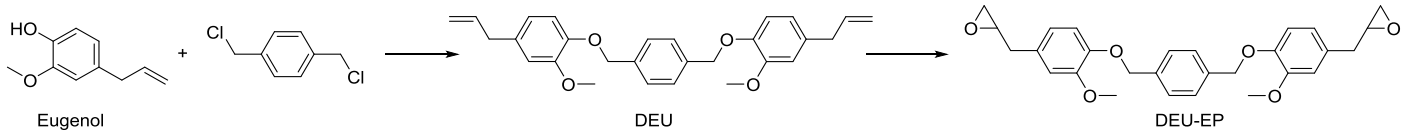

Scheme 1. Synthesis of eugenol-based epoxy resin (DEU-EP).

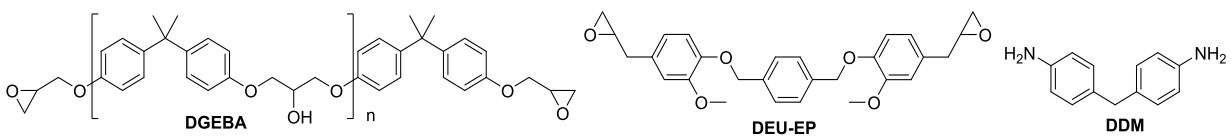

Scheme 2. Molecular structures of DGEBA, DEU-EP and DDM used in this study.

2. Experimental section

2.1 Materials

Eugenol (4-allyl-2-methoxyphenol), α,α'-dichloro-p-xylene, anhydrous potassium carbonate, N,N-dimethylformamide, meta-chloroperoxybenzoic acid (~77%, mCPBA), dichloromethane, sodium hydroxide, and sodium sulfite were purchased from the Sigma-Aldrich Company. Pristine bisphenol A epoxy resin (DGEBA) with the epoxy value of 0.422 mol/100g was obtained from Nantong Xingchen Synthetic Materials Co. Ltd., China whose ^{1}H-NMR, ^{13}C-NMR and GPC curves are given in Supporting information (Figs S3-5), and curing agent 4,4'-diaminodiphenyl methane (DDM), was obtained from TCI Europe Company. Other chemicals and solvents were commercially available and used as received. The eugenol-based epoxy resin (DEU-EP) was synthesized in our lab whose molecular structures of the epoxy resins along with the bisphenol A epoxy resin (DGEBA) and curing agent used in this study are given in Scheme 2. Note here that there may be an alternative way to epoxide the double bond of DEU-EP, for example H_2O_2/acetic acid; however, mCPBA is more direct for lab-scale synthesis of a small amount of samples, and reaction condition is very mild and easy to well control.

2.2 Synthesis of eugenol-based epoxy resin (DEU-EP)

As shown in Scheme 1, DEU-EP was synthesized from the Williamson etherification reaction between α,α'-dichloro-p-xylene and eugenol to yield intermediate bearing two allyl groups, followed by epoxidation of the allyl double bonds by meta-chloroperoxybenzoic acid (mCPBA). The detailed procedures are as follows.

Into a 500 ml round-bottomed flask, α,α'-dichloro-p-xylene (35g, 0.20 mol), eugenol (78.8 g, 0.48 mol) and K_2CO_3 (66.3, 0.48 mol) were charged, and 210 ml DMF was added with continuous stir. The reaction progressed at room temperature for 6 hours and then at 60 ^{o}C for 3 days. After that, the obtained slurry was poured into a large amount of water and stirred for two hours. After filtration, slightly yellow solid resulted, and then was washed with 5% NaOH water solution, deionized water, and ethanol to yield white crystal in sequence. The crystal was dried at 100 ^{o}C in vacuum for two hours to yield 83.2 g of titled compound (DEU) in excellent isolated yield (96.6%). Mp (DSC onset temperature) =106 ^{o}C. FTIR (KBr): 3080 cm^{-1} and for anti-symmetric stretch of allyl C-H bond, 3060, 3040 and 3002 cm^{-1} for benzene and epoxy ring C-H stretch, 2873 for 2940 cm^{-1} for CH_3 and CH_2 respectively, 1607, 1511 and 1449 cm^{-1} for benzene ring stretch, 1034 cm^{-1} due to the C-O-C stretch, 1638 cm^{-1} and 903 for C=C double stretch and out-of-plane bend. ^{1}H-NMR (400 Hz, $CDCl_3$): 3.28 ppm (4H), C*H*$_2$-CH=CH$_2$; 3.82 ppm (6H), OC*H*$_3$; 5.00-5.02 ppm (4H), CH=C*H*$_2$ and PhC*H*$_2$-, 5.89 ppm (2H), C*H*=CH$_2$, 6.62-6.76 ppm (6H), CH$_2$=CH-CH$_2$-Ph (*H*); 7.37 ppm (4H), CH$_2$-Ph(*H*)-CH$_2$. ^{13}C-NMR (101 Hz, $CDCl_3$): 40.1 ppm, *C*H$_2$-CH=CH$_2$; 115.9 ppm, CH$_2$-CH=*C*H$_2$;

137.9 ppm, CH_2-*C*H=CH_2; 115.9 ppm and 56.2 ppm, O*C*H_3; 71.2 ppm, Ph*C*H_2-O; 112.6 ppm; 114.5 ppm, 120.7 ppm, 133.6 ppm, 146.7 ppm and 149.8 ppm Ph-CH_2-O-Ph(C); 127.7 ppm, 137.2 ppm, Ph(*C*)-CH_2O.

40.0 g of DEU was dissolved into CH_2Cl_2 (600 ml) at 5 ^oC, and then 50 g of meta-chloroperoxybenzoic acid was added to the mixture. The reaction mixture was stirred at room temperature for one day. After that, the formed solid by produced was filtered off at 0 ^oC, then other amount of mCPBA (23.5g) was added and stirred at room temperature for another 7 days. After that, cool the mixture to 0 ^oC, and then the white solid byproduct was filtered off. Then 50 g of Na_2SO_3 in 250 ml water was added and stirred at room temperature for two days to yield two-layer liquid. After removal of solvent and dried in vacuum at 40 ^oC overnight, the obtained yellow solid product was digested in a 200 ml ethanol and stirred overnight to yield white to slight yellow powder. This product was washed with deionized water and ethanol, and finally dried at 80 ^oC under vacuum overnight to yield DEU-EP (19.0 g, 44.2%) which could crystallize from ethanol to form needle crystal. The epoxy value of (DEU-EP) is 0.380 mol/100g determined with titration according to ASTM D1652-04 ($HClO_4$/acetic acid method). Melting point (DSC onset) = 124 ^oC. DEU-EP FTIR (KBr): 3058 cm^{-1} for benzene ring C-H stretch, 2874 cm^{-1} for 2927 for CH_3 and CH_2 respectively, 1608 and 1514 cm^{-1} for benzene ring stretch, 1130 and 1030 cm^{-1} due to the C-O-C stretch; 926 and 856 cm^{-1} for epoxy ring vibration and 1260 cm^{-1} for epoxy ring symmetric stretch. ^{1}H-NMR (400 Hz, $CDCl_3$): 2.54-3.12 ppm (10H), C*H*$_2$-C*H*-C*H*$_2$ (epoxy ring); 3.88 ppm (6H), OC*H*$_3$; 5.13 ppm (4H), PhC*H*$_2$-; 6.72-6.82 ppm (6H), Ph(*H*); 7.42 ppm (4H), CH_2-Ph(*H*)-CH_2. ^{13}C-NMR (101 Hz, $CDCl_3$): 38.6ppm, CH_2-epoxy; 47.5 and 54.5 ppm, Epoxy (2C); 56.2 ppm, -OCH_3; 71.1 ppm, Ph*C*H_2-O; 113.1 ppm, 114.4 ppm, 121.2 ppm 130.7 ppm, 147.1 ppm, 149.8 ppm epoxy-CH_2Ph(6C); 127.7 ppm, Ph(4C)CH_2O; 137.1 ppm, Ph(2C)CH_2O.

2.3 Gel permeation chromatography (GPC)

A Waters gel permeation chromatography (GPC) was used to determine the molecular weight and its distribution. GPC consists of a 1525 HPLC pump, a 2414 refractive index detector, a 2489 UV/Visible detector, a 1500 column heater, and a series of GPC columns (Styragel HR 0.5, 2.0, 3.0 and 4.0). THF was used as the solvent with flow rate of 1 ml/min, and the calibration curve was established with polystyrene standards.

2.4 Differential scanning calorimetry (DSC)

Curing reactions of DGEBA/DDM and DEU-EP/DDM systems were investigated using a differential scanning calorimeter (DSC 200, TA Instruments, USA) with an intercooler. DEU-EP and curing agent (DDM) according to the ratio of epoxy to amine hydrogen of 1:1 were mixed and pulverized in an agate mortar to achieve a homogenous fine

powder, and then dried in vacuum at 40 °C for two hours. For the controlled experiment, DGEBA and DDM were dissolved in dichloromethane, and then the solvent was removed in high vacuum at 40 °C for two hours. The epoxy curing mixture was transferred into an aluminum DSC crucible ready for testing. For a nonisothermal run, the heating rate was 10K/min, and the temperate ranged from 0 to 300 °C. For an isothermal run, the epoxy reaction mixture was heated quickly (100 °C/min) to the curing temperature of 120, 125, 135 and 140 °C, and held isothermally until no reaction exotherm observed. The sample weight was 10-12 mg and all the DSC runs were carried out in dry N_2 flow (50 ml/min).

2.4 Preparation of the cured epoxy sample

DGEBA or DEU-EP was mixed well with curing agent (DDM) in the stoichiometric balance (molar ratio of epoxy groups to amino hydrogen = 1:1) at 120 °C in oil bath for a few minutes, and then poured into a preheated silicone rubber mould immediately. The curing reaction progressed at 140 °C for 5 hours in air. This curing produce could ensure the both ensure the complete cure to allow the two systems to well cured state without thermal degradation. After demoulding, the specimens were obtained and polished for the further test.

2.5 Dynamic mechanical analysis (DMA)

A dynamic mechanical analyzer (DMA Q800, TA Instruments) was used to study the thermomechanical properties of the cured epoxy resins. The rectangular specimens were fastened on a single cantilever clamp (length = 17.50 mm, width = 12.0 ± 1.0 mm, thickness = 2.80 ± 0.20 mm), the heating rate was 3 °C/min, and the oscillation frequency was 1Hz. The temperature ranged from room temperature to well above the glass temperature.

2.6 Nanoindentation mechanical property analysis

A Hysitron TI 950 nanoindentation system equipped with a Berkovich diamond indenter was used to study the mechanical properties of the cured epoxy resins. During testing, load-displacement profiles were recorded and then used to calculate the hardness, Young's (elastic) modulus and creep displacements [30]. This technique has been successfully used to analyze mechanical properties of the cured epoxy resins [31-33]. Here the cured epoxy resins were metallurgically prepared to ensure the very smooth surface, and then dried in vacuum at 40 °C overnight. The maximum indentation load was 9 mN, with the loading and unloading rate of 300 and 450 μN/s, respectively. The dwell time at the maximum indentation load was 5 s. The spacing of each discrete indent was larger than 100 μm, and minimum of 36 discrete indentations were conducted on the same sample. To evaluate the creep resistance of the

sample, the peak indentation load, loading rate and unloading rates were fixed at 9 mN, 300 μN/s and 450 μN/s, respectively. The relatively long dwell time (600 s) for the maximum force was used, and the instrument thermal drift rate was within 0.03 nm/s for sieving effective indents.

2.7 Thermogravimetric analysis (TGA)

A thermogravimetric analyzer (TGA, TA Instruments, USA) was used to study the thermal decomposition of cured epoxy resins. The heating rate was 10 ^{o}C /min, temperature ranged from room temperature to 750 ^{o}C, the protection gas was dynamic dry N_2 (40 ml/min), and the weight of the samples was approximately 10 mg.

2.8 Micro calorimeter flammability test

Microscale combustion calorimetry (MCC, Fire Testing Technology, UK) is a convenient technique used in recent years for the investigation of flammability of polymers. In this study, MCC was used to investigate the flammability of cured epoxy resins according to ASTM D7309. About 5 mg sample was heated to 700 ^{o}C with a heating rate of 1 ^{o}C/s at a stream of nitrogen flowing at 80 cm^3/min. The volatile and anaerobic thermal degradation products in the nitrogen stream are mixed with a 20 cm^3/min stream including 20% oxygen and 80% nitrogen prior to entering a combustion furnace at 900 ^{o}C.

2.9 Horizontal burning test

The horizontal burning tests were conducted on the cured epoxy resins. The specimens with thickness of 3 mm and width of 10 mm was fixed on a clamp horizontally, and the front of the specimen was ignited (10s). The standard burner (blue flame) was used according to ASTM D5025. The entire burning process was recorded using a digital video recorder.

3. Results and discussion

3.1 Synthesis of intermediate and epoxy resin

We develop a facile approach (Scheme 1) to prepare the eugenol-based epoxy resin (DEU-EP) in which two steps are involved: (1) the Williamson ether reaction between α,α'-dichloro-p-xylene and eugenol to yield intermediate (DEU) bearing two allyl groups, and (2) the epoxidation of the allyl groups to yield DEU-EP. DEU was synthesized with K_2CO_3 as the acid absorber under mild conditions (DMF/60 ^{o}C). The isolation method of DEU is also very

simple by just by washing with sodium hydroxide water solution, ethanol, water and the yield is very high (96.6%). More attractively, as mentioned in the introduction section, eugenol can be obtained from biobased essential oils. As another synthesis material of DEU, α,α'-dichloro-p-xylene shows the great potential to be produced via a biobased route.

DEU was used to synthesize the epoxy resin by epoxidation of its double bonds using excessive mCPBA in dichloromethane in one step at room temperature. The final epoxy product (DEU-EP) was isolated by digesting the raw product in ethanol to yield white solid powder and then wash with water. Although there is still a big room to further increased the accumulated yield of DEU-EP (currently 44%) by optimizing the reaction conditions (e.g., using other epoxidation processes), our method avoids the column chromatography for purification of the final product in good purify, which greatly simplify the isolation process. Moreover, from a molecular structure point of view, even without considering the possibility of its p-xylene moiety from renewable feedstock, DEU-EP still maintains 70.2% of the original eugenol weight higher than that of the previously reported epoxy resin (62.7%) derived from the direct epoxidation of the allyl and phenolic hydroxyl group of eugenol [25]. Therefore, our molecular design can introduce increased amount of eugenol segments into DEU-EP, which will benefit to take full advantage of eugenol in epoxy chemistry.

Fig. 1.

Fig. 1a compares the ^{1}H-NMR spectra of the intermediate (DEU) and synthesized epoxy resin (DEU-EP). The double-related protons of DEU appear around 5.00-5.89 ppm corresponding to the hydrogen atoms at different positions in different configurations, while the signal at 3.2 ppm is due to the methoxyl group. After epoxidation of the double bonds, the signals for double bond disappear, which is also supported by the disappearance of IR absorption due to the stretch of C=C double bonds at about 1638 cm^{-1} and out-of-plane bend of $=CH_2$ at about 931 and 1863 cm^{-1} (Supporting information Fig. S4). Meanwhile, the signals related to the epoxy ring and its adjacent substituents appear at 2.54-3.12 ppm corresponding to the hydrogen at different positions in different configurations. Moreover, in the ^{13}C-NMR spectrum (Fig. 1b) of the final epoxy resin, signals for the different carbon atoms of DEU-EP can be identified. The agreement of ^{1}H-NMR, FTIR and ^{13}C-NMR spectra with its expected molecular structure of DEU-EP. Furthermore, the relative molecular weight and its distribution of eugenol and DEU-EP are shown in Fig. 3c. DEU-EP shows a shorter retention time than Eugenol, which indicates the increased molecular weight of DEU-EP. The determined the number average of DEU-EP and eugenol (428 and 158) is rather close to their ideal molecular weight

(462 and 164), and molecular weight distribution of DEU-EP is very close 1. These results can be give further support the achievement of DEU-EP.

3.2 Nonisothermal cure of epoxy resin

The curing reaction of DEU-EP with stoichiometric 4,4'-diaminodiphenyl methane (DDM) was studied and compared to DGEBA from nonisothermal DSC analysis. Fig. 2 displays the nonisothermal DSC thermal analytic curves of DGEBA/DDM and DEU-EP/DDM. DGEBA/DDM shows a single thermal curing process with a strong exothermic peak (T_{peak} = 161 ^{o}C). In contrast, DEU-EP/DDM shows three major thermal events: melting of DDM with T_{peak} at 80.1 ^{o}C, melting of DEU-EP and exothermic cure of the epoxy system (T_{peak} = 166 ^{o}C). The higher T_{peak} of DEU-EP/DDM indicates the lower the reactivity of DEU-EP compared to DGEBA. The lowered reactivity is due to the less delocalized electron cloud on the epoxy group of DEU-EP compared with that of DGEBA, which makes the nucleophilic addition of the amine group to the epoxy ring more difficult. However, difference in the reactivity of DEU-EP and DGEBA is not significant, when DDM is used as the curing agent, which indicates that DEU-EP has the high curing reactivity.

Fig. 2.

The overlap of endothermic melting and exothermic curing reaction makes the nonisothermal analytic curves of DEU-EP/DDM rather complex, which is unsuitable to curing kinetic analysis because we cannot clearly determine the baseline for the integration of exothermic peak. Despite that, DEU-EP/DDM system is stable at room temperature and the curing reaction will be activated thermally upon heating to the melting temperature range of DDM and DEU-EP. In other words, DDM (M_p = 89-90 ^{o}C) and DEU-EP and have the melting points much higher than room temperature (Supporting information, Fig. S5), so that they will not react each other at room temperature with long storage life. This finding likely implicates that DEU-EP/DDM has the potential in epoxy powder coatings with long storage life at room temperature and a fast enough curing reaction rate upon heating to melt the epoxy system.

3.3 Isothermal curing behaviors and kinetic molding

To better understand the curing behavior the DEU-EP/DDM, we examined its isothermal curing reaction. Fig. 3a compares the isothermal curing reaction (140 ^{o}C) of DEU-EP/DDM and DGEBA/DDM, displaying the heat flow and

fractional conversion as a function of time. DEU-EP/DDM shows a lower exothermic peak value than DGEBA/DDM (-0.3981 W/g vs. -0.6057 W/g), and the former shows slower increase in conversion with time. These results approve the lowered reactivity of DEU-EP/DDM, and agree well with the conclusion drawn from the nonisothermal curing reaction analysis (Fig. 2). Nevertheless, if the curing time is sufficient long, the final conversion of the two systems are very close. Furthermore, DEU-EP/DDM and DGEBA/DDM show very close averaged reaction heat (307.8 ±7.6 J/g vs. 309.6 ±12.9 J/g). These results indicate that both systems can reach essentially the same ultimate conversion at curing temperature 140 ^{o}C. Therefore, DEU-EP has high enough reactivity to be well cured by a typical aromatic amine curing agent (DDM).

Fig. 3.

To understand the curing reaction of DEU-EP/DDM in quantitative way, we conduct the isothermal curing reaction kinetic analysis to avoid the exothermic curing and endothermic melting of the epoxy resin and curing agent. Fig. 3b gives the DSC analysis and conversion curves of the isothermal curing reaction of DEU-EP/DDM at the temperature of 120, 125, 135 and 140 ^{o}C. In this temperature range, melting of the DDM and DEU-EP result in initial reaction system at a liquid stat, and the interference of melting of DDM and TEU-EP can be neglected (Fig 2a). Moreover, it this temperature range the curing rate of the DEU-EP/DDM is relatively low and the reaction time is relatively long. In this case, the influence of the equilibrium time before reaching the isothermal temperature is trifle and neglectable. The exothermic peak appears at time ($t > 0$), which means the isothermal reaction reaches its maximum rate at an intermediate curing stage due to the autoacceleration of the curing reaction. Increasing temperature leads to the systematically increased exothermic peak and thus the curing rate.

After transforming the fractional conversion-time data to the reaction rate as a function of the conversion, as shown in full lines (Fig. 4), we can find the maximum reaction rate occurs at the essential same conversion (~15%). This remake indicates that the curing reaction is autocatalytic, and within the experiment temperature range, the temperature will little affect the autocatalytic reaction mechanism. As illustrated in Scheme 3, the autocatalytic reaction mechanism results from the hydroxyl groups generated from the epoxy-amine ring-opening reaction that can catalyze the further curing reaction via a trimolecular transition state [34, 35].

Fig.4.

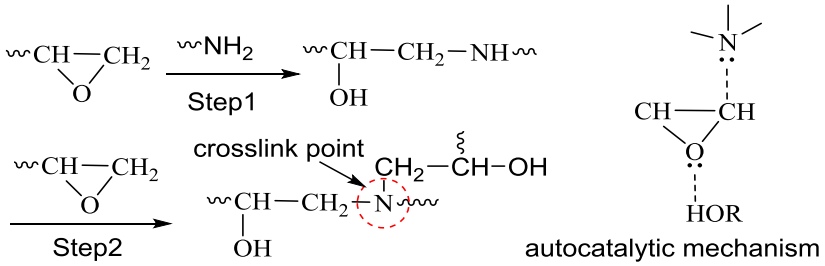

Scheme 3. Epoxy-primary amine curing reactions and epoxy-amine-hydroxyl group trimolecular transition state for the autocatalytic mechanism of epoxy amine curing reaction.

$$\frac{d\alpha}{dt} = \left[k_1(T) + k_2(T)\alpha^m\right](1-\alpha)^n \quad (1)$$

Taking the autocatalysis into account, we use two-parameter autocatalytic Kamal model [36] (Eq. (1)) to simulate curing reaction rate of DEU-EP/DDM In this equation, $k_1(T)$ is the non-autocatalytic rate, $k_2(T)$ is the autocatalytic rate, α is the conversion, and m and n are the respective reaction orders of the non-autocatalytic and autocatalytic reactions. Here k_1 is estimated by extrapolating the initial conversion (0.02-0.05) to zero to yield intercept that can give rise to the k_1 value, and the other parameter, k_2, m and n, can be estimated by fitting the experimental conversion-curing rate data using a nonlinear fitting tool of the Origin software [37, 38]. The obtained kinetic parameters in the Kamal model (Table 1) shows that k_1 and n are much higher than k_2 and m, which implicates that the autocatalytic reaction processes at a much faster than the nonautocatalytic reaction.

Table 1. Parameters of the Kamal model for DEU-EP/DDM at the curing temperature (T_c) of 120, 125, 135, and 140 °C. k_1, k_2, m and n are the rate constants and reaction orders for nonautocatalytic and autocatalytic reactions, respectively. SE is the standard error and R2 is the squared correlation coefficient of nonlinear fitting.

Tc(°C)	k_1(min^{-1})	SE	k_2(min^{-1})	SE	*m*	SE	*n*	SE	R^2
120	0.02287	5.69×10^{-5}	0.05283	4.76×10^{-5}	0.58811	0.00429	1.67573	0.00468	0.99317
125	0.03084	7.91×10^{-5}	0.06278	3.25×10^{-4}	0.42382	0.00233	1.65546	0.00311	0.99622
135	0.04897	1.62×10^{-4}	0.10085	2.73×10^{-4}	0.29774	0.00113	1.68266	0.00202	0.99700
140	0.06091	1.90×10^{-4}	0.12329	3.47×10^{-4}	0.25779	0.00115	1.66514	0.00225	0.99607

As the curing temperate increases, n is almost unchanged, but m decreases gradually, which indicates that autocatalytic reaction is less dependent on the curing temperatures. Note that k_2 and n are much greater than k_1 and m, which implicates that autocatalytic reaction plays a much more important role in the curing kinetics of DEU-EP/DDM, and the curing rates are mainly determined by the autocatalytic behavior of the system [34]. Using the Kamal model

and kinetic parameters (Table 1), we can obtain the simulated reaction rate-conversion curves (Fig. 4) which are in excellent agreement with the experimental ones. Therefore, the Kamal model can well describe the isothermal curing rate of DEU-EP/DDM.

In addition, using of k_1 and k_2 values in Table 1, the Arrhenius plots of ln k_1 and ln k_2 vs. 1/T are constructed in Fig. 5 showing the excellent linear interdependency. As a result, the activation energies for the nonautocatalytic and autocatalytic reactions, E_{a1} and E_{a2}, can be calculated from the well-known classic Arrhenius law. E_{a1} is larger than E_{a2} (65.4 ± 2.2 kJ/mol vs. 58.6 ± 2.3 kJ/mol); therefore, the autocatalytic curing reaction has a lower energetic barrier than the nonautocatalytic curing reaction. The identified autocatalytic curing reaction shows a lower activation energy, because the hydroxyl group generated in the epoxy-amine addition reaction catalyzes the further epoxy-amine curing reaction via a trimolecular transition state with a lowered energetic barrier (Scheme 3).

Fig. 5.

3.4 Isoconversional analysis of the isothermal curing kinetic mechanisms

To reach a deeper insight in the kinetic mechanisms of the isothermal curing reaction of DEU-EP/DDM, we conduct the isoconversional analysis on the curing reaction of DEU-EP/DDM. Isoconversional analysis based on the basic principle that states that the kinetic rate at constant extent of conversion is only a function of temperature, and the previous reports has showed that isoconversional analysis is very useful for mechanism and kinetic analysis of curing reaction of epoxy resins based on thermal analytic data [39-41]. Herein, we apply the advanced isoconversional method (the Vyazovkin method) to calculate of effective activation energy for the different conversions. The effective activation energy E_α can be determined for any specific α by minimizing Eq. (2a):

$$\Phi\left(E_\alpha\right)=\sum_{i=1}^{n}\sum_{j\neq i}^{n}\frac{J\left[E_\alpha,T_i\left(t_\alpha\right)\right]}{J\left[E_\alpha,T_j\left(t_\alpha\right)\right]}=\min \quad (2a)$$

$$J\left[E_\alpha,T_i\left(t_\alpha\right)\right]\equiv\int_{t_{\alpha-\Delta\alpha}}^{t_\alpha}\exp\left[\frac{-E_\alpha}{RT_i\left(t\right)}\right]dt \quad (2b)$$

where subscripts, *i* and *j*, denote the different experiments with different heating programs, $\Delta\alpha$ indicates the small increment in conversion (0.02), and integral *J* in Eq. (2b) can be evaluated numerically with a trapezoid rule. Repeat this minimization procedure for each α, and eventually an E_α-α relationship result (Fig. 6).

Fig. 6.

As shown in Fig. 6, at the very beginning of the cure E_α (~64 kJ/mol) is very close to E_{a1} (~65.4 kJ/mol) in the autocatalytic Kamal model; see Fig. 5. This E_α value can be ascribed to the nonautocatalytic reaction between the epoxy group of DEU-EP and the primary amino group of DDM (Scheme 3). As the conversion increases, E_α decreases gradually, likely due to the increasing number of the secondary hydroxyl groups [42] in the reaction system formed during curing reaction. The accumulation these hydroxyl groups leads to more and more pronounced autocatalytic reaction, thus showing lower activation energy in the overall curing kinetics. On the other hand, as the reaction progresses, the concentration of the primary amino group from DDM decreases steadily, and formed secondary amino groups increases gradually first and decreases monotonously at the high-conversion stage. In this case, the reaction between epoxy groups and secondary amine group has a higher activation energy due to the increased steric hindrance, which results in a slight increase in E_α occurs after the 80% conversion. In this case, reaction between epoxy and secondary amino group reaction likely dominates the curing kinetics.

In the deep cure stage ($\alpha > 80\%$), E_α decreases again, which likely indicates that the diffusion process of reactive species affects the curing kinetics to a varying extent, because the concentrations of the reactive epoxy and amine groups is very low. Specially, the *p*-xylene ether bonds of DEU-EP/DDM will facilitate the diffusion of epoxy groups to effectively collide with reactive amine groups to react with each other, since these bonds are relatively easy to rotation with much lower activation energy, in analogy to the other thermosetting curing reactions [43]. Therefore, we observe the decrease in E_α at the final stage of the isothermal cure.

In summary, DEU-EP/DDM shows a complicated reaction mechanisms affected by not only the pure chemical reaction but also the diffusion process of the reactive groups at the difference curing stages.

3.5 Dynamical mechanical properties of epoxy resin

The dynamic mechanical properties of the cured DEU-EP/DDM and DGEBA/DDM were studied in a comparative way. Fig. 7 displays the obtained DMA spectra for storage and loss modulus and Tan δ against temperature. Fig. 7a shows that DEU-EP/DDM exhibits higher storage modulus (E') than DGEBA/DDM up to 97 ^{o}C, in particular, near the room temperature range. For example, the E' value of DEU-EP/DDM is 18% higher than that of DGEBA/DDM (2629 ± 28 MPa vs. 2252 ± 40 MPa (30 ^{o}C)), see Table 2. The increased E' value means under a given load the network will deform elastically to a decreased extent, and therefore the DEU-EP can endow the cured epoxy resin with higher stiffness than DGEBA when used as the hard plastics near room temperatures. On the other hand, Fig. 7b shows at DEU-EP/DDM network has much higher loss modulus (E") than DGEBA/DDM (e.g., 76.6 ± 5.4 MPa vs. 31.4 ± 1.3

MPa (30 °C)), which indicates that much more elastic energy will be absorbed at the glassy state of the network and converted to heat. The increased E" value could be attributed to the plastic motion of the *p*-xylene ether bonds in the glassy network, which will positively contribute to prevent the vibration and impact damage of the cure epoxy materials near room temperature range by converting these mechanical energy to heat.

Fig. 7.

Once the temperature increases over 97 °C, the storage modulus (E') of DEU-EP/DDM decreases faster than that of DGEBA/DDM and shows a lower E' value. The glass temperature (T_g) for Tan δ of the former is lower than that of the latter (114.4 ± 0.3 °C vs. 153.6 ± 2.2 °C); see Fig. 7a and Table 2. Decreased E' and T_g are likely due to the *p*-xylene ether bonds in the DEU-EP/DDM network which increase the flexibility of the network chain at a higher temperature. Moreover, the methoxyl groups inherent from eugenol may further increase the free volume in the cured epoxy networks, which will further decrease the glass temperature.

Table 2. Glass relaxation temperatures, peak height and width, characteristic storage and loss modulus of DGEBA/DDM and DEU-EP/DDM networks determined from Fig. 7.

Formulation	DGEBA/DDM	DEU-EP/DDM
Glass-relaxation (Tan δ)/ °C	153.6 ± 2.2	114.4 ± 0.3
Peak height of Tan δ	0.923 ± 0.02	1.168 ± 0.10
Peak height of loss modulus/MPa	286.6 ± 14.1	362.0 ± 33.8
Peak width of half height/°C	14.5 ± 0.3	14.0 ± 1.0
Storage Modulus at 30 °C/MPa	2252 ± 40	2629 ± 28
Loss Modulus at 30 °C/MPa	31.4 ± 1.3	76.6 ± 5.4
Storage Modulus at 60 °C/MPa	2082 ± 48	2415 ± 41
Loss Modulus at 60 °C/MPa	38.7 ± 3.5	62.1 ± 2.4
Storage Modulus at 97 °C/MPa	1868 ± 29	1877 ± 28
Loss Modulus at 97 °C/MPa	39.9 ± 6.1	108.8 ± 11.1
Crosslink density (mol/m^3)	2285 ± 153	1346 ± 113

Nevertheless, at a lower temperature, especially near room temperature range, the higher E' value of DEU-EP/DDM likely suggests that the stronger interaction in the cured network. This interaction is probably owing to the more

regular packaging of the aromatic moieties in the DEU-EP/DDM epoxy network (Scheme 4) resulting optimally compacted configuration of the network chains, which creates stronger cohesive energy (e.g., π-π stacking among the aromatic rings) in the network at the glassy state [44-46]. However, this non-covalent becomes very weak, once the *p*-xylene ether bonds possess enough kinetic energy to overcome the energetic barrier for their motions at a higher temperature. In this case, the E' value for DEU-EP/DDM decreases dramatically, especially in the glass-rubber transition range. Our result also indicates that increased glass temperatures of the epoxy networks will not necessarily result in their enhanced rigidity especially at a relatively low temperature range.

The crosslink density are estimated from well-known rubber elastic theory, Eq. (3):

$$E_r = 3RT_r v_e \quad (3)$$

where R is the universal gas constant, T_r is well above the glass temperature, the temperature storage modulus is noted as to E_r, and v_e is the crosslink density. Table 2 shows that the DEU-EP/DDM show a lower crosslink density than DGEBA/DDM (2285 ± 153 mol/m^3 vs. 1346 ± 113 mol/m^3). The decreased crosslink density is unlikely due to the chemical crosslinks but interaction between the molecular chains, because the epoxy value of DGEBA and DEU-EP differ less significantly (only about 10%) and the both system can reach the well-cured state. The decreased crosslink density of DEU-EP/DDM should be attributed to the other reasons, as detailed below.

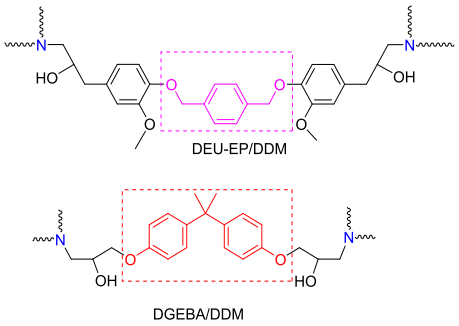

Scheme 4. Schematic illustration of network structures of cured DEU-EP/DDM and DGEBA/DDM networks.

In the DGEBA/DDM network, the more rigid bisphenol A moieties seem to play a much important role in keeping the rigidity of network at a higher temperature, due to difficulty in chain motions (relatively short and more rigid). In contrast, for the DEU-EP/DDM network where the aromatic rings inherent from eugenol are linked by the *p*-xylene ether bonds (long and more flexible), once the motion of these ether bonds is restricted at a lower temperature, the epoxy network will show higher storage modulus. However, once the motion of *p*-xylene ether bonds are sufficiently activated at a higher temperature, the motion of their linked eugenol and *p*-xylene segments will become easier than

that of the bisphenol A moieties from the DGEBA/DDM networks (Scheme 4), thus resulting in lower modulus, especially in the rubber state.

In addition, DEU-EP/DDM shows higher peak values for Tan δ and loss modulus (E") values than DGEBA/DDM during the glass transition process, which indicates that the increased elastic energy dissipation in the former network (Fig. 7b and Table 2). The reason for this finding is as follows. The *p*-xylene ether bonds and the methoxyl groups inherent from eugenol increase the viscous deformation (plastic deformation) ability of the network during the glassy relaxation process.

In summary, eugenol turns out to be a very useful building block to construct epoxy resins with higher stiffness than bisphenol A epoxy resins in a certain temperature range.

3.6 Nanoindentation analysis of cured epoxy

Nanoindentation was used to evaluate the mechanical properties of the cured epoxy resins including Young's (elastic) modulus, hardness and creep resistance. To avoid the 'skin effect' due to the absorption between polymer matrix and indenter during the test [47] a relatively large peak load was used, resulting in large indention depth, above 1 μm. Representative load-displacement curves of DGEBA/DDM and DEU-EP/DDM are shown in Fig. 8a. DGEBA/DDM shows a larger displacement than that of DEU-EP/DDM at the same load, which indicates that the DEU-EP/DDM network shows a higher resistance to the indenter penetration with a maximum indentation displacement, h_{max}, at 9000 μN of 1311 nm, while the DGEBA/DDM network shows the lower resistance to penetration, with a higher h_{max} of 1368 nm. The increased indentation resistance is due to the higher rigidity the cured DEU-EP/DDM network. DEU-EP, consisting of the highly concentrated and regular arranged aromatic ring subunits, will lead to stronger Van der Waals forces such as π-π stacking among the aromatic rings in the cured epoxy network at room temperature. Therefore, the network shows higher indentation resistance. The hardness (H) and Young's modulus (E) of the cured epoxy resins were determined following standard procedures found elsewhere [31]. The obtained H and E values of the DGEBA/DDM and DEU-EP/DDM networks are compared in Fig. 8b. DEU-EP/DDM shows 20% increase in the Young's modulus and 6.7% increase in the hardness compared with DGEBA/DDM. Thus, DEU-EP/DDM has more attractive room-temperature mechanical properties than DGEBA/DDM.

Fig. 8

The cured epoxy resins were indented with a constant load of 9.0 mN for 600 s after the initial loading to examine the creep behavior. The registered creep displacements as function of time for the DGEBA/DDM and DEU-EP/DDM are compared in Fig. 9. Initially, the two creep curves coincide, but extending testing time leads to dramatic changes between the curves. DEU-EP/DDM shows a higher creep displacement than DGEBA/DDM, with a 36% increase in the creep displacement at 600 s. The increased creep displacement indicates the enhanced motions of polymeric chains in the DEU-EP/DDM network. This observation likely indicates that the *p*-xylene ether bonds and the methoxyl groups inherent from eugenol promote the motion of related chains in a relatively long time scale, which agrees with the much increased loss modulus based on DMA results (Fig. 7b). The enhanced motions of the network chains will benefit to release the interior stress in the materials, and thus increases the failure resistance. The high elastic modulus and hardness combined with increased ability of chain motion make DEU-EP attractive for many important applications where high stiffness and toughness are particularly important.

Fig. 9.

3.7 Thermal decomposition of cured epoxy resin

The thermal decomposition process of the cured DEU-EP/DDM was studied and compared to DGEBA/DDM based on thermogravimetric analysis (TGA). Fig. 10 displays the weight percentage and derivate weight percentage (TG and DTG) against temperature. TG curves show that DEU-EP/DDM and DGEBA/DDM are thermally stable up to 270 ^{o}C without marked mass loss observed. As the temperature further increases, DEU-EP/DDM begins to decompose, whereas DGEBA/DDM starts to decompose at a higher temperature (~320 ^{o}C). For 5% weight loss, DGEBA/DDM shows a higher temperature than DEU-EP/DDM (379 ^{o}C vs. 341 ^{o}C). The initial lower decomposition temperature of DEU-EP/DDM is attributed to the detachment of the methoxyl groups inherent from the eugenol-moieties [48]. In this case, we hope that if we can convert these methoxyl groups into another more thermally stable ones, which will be great benefit to the thermal stability of the resulting materials. In the temperature range of 350-500 ^{o}C, DGEBA/DDM and DEU-EP/DDM decompose rapidly reaching their respective maximum rates at 393 ^{o}C and 377 ^{o}C. Interestingly, the maximum decomposition rate of DEU-EP/DDM is much lower than that of DGEBA/DDM (0.8632 %/^{o}C vs.1.736 %/^{o}C), which suggests the sluggish decomposition of the former network to form volatile gases.

Fig. 10.

More impressively, DEU-EP/DDM shows an unexpected high char yield of 38% (700 ^{o}C) which is 2.11 folds of the char yield of DGEBA/DDM (18%) at the same temperature. Such high char yield is unusual in the epoxy systems without any flame retardant and/or element functional groups (e.g., phosphorous-contained moieties). This finding also implicates that much reduced flammability of cured EDU-EP/DDM relative to DGEBA/DDM, because the less combustible releases via increased charring of the epoxy matrix. The high char yield of EDU-EP/DDM is associated with p-xylene dimethyl ether-linked aromatic rings from eugenol in the DEU-EP/DDM network. These units tend to transform to the *p*-xylene methane-linked aromatic structure that will promote charring of the epoxy matrix after high-temperature pyrolysis. This result is analogue to the previous report on thermal decomposition of hexamethylenetetramine-cured phenolic novolac resins, where methane-linked phenolic rings resulted in very high char yield (>50% at 800 ^{o}C) after high-temperature pyrolysis [49]. In summary, DEU-EP/DDM has the sufficient thermal stability relative to its glass temperature (114.6 ^{o}C), and exhibits very low decomposition rate and high char yield after high-temperature pyrolysis.

3.8 Flammability of cured epoxy resin

As the discussed above, the very high char yield of DEU-EP/DDM is expected to result in lower the flammability of the materials. To be quantitative, microscale combustion calorimetry (MCC) was used to examine the flammability of the cured epoxy. MCC is a relatively new and rapid method to evaluate flammability of materials, taking the advantage of small sample requirement (on milligram quantities) [50]. Fig. 11 presents the typical MCC curves for heat release rate (HRR) vs. temperature along with the values of the average peak heat release rate (PHRR), total heat release (THR) and peak heat release temperature (T_{peak}) for both of DEU-EP/DDM and DGEBA/DDM systems. The results show that although DEU-EP/DDM and DGEBA/DDM exhibit a closer PHHR temperature, DEU-EP/DDM shows a much lower PHRR value than DGEBA/DDM (201 ± 7 W/g vs. 447 ± 18 W/g), a reduction in the PHHR value by 55%. Furthermore, the THR values of two systems are quite different. DEU-EP/DDM shows a much lower THR value than DGEBA/DDM (16.3 ± 0.8 kJ/g vs. 26.6 ± 0.9 kJ/g), a reduction in THR by 38%. These data suggest that flammability of DEU-EP/DDM is less intensive than that of DGEBA/DDM under the same combustion condition.

Fig. 11.

The reduced flammability is also associated with the unique molecular structure of DEU-EP compared to DGEBA. To illustrate, during the pyrolysis of DEU-EP/DDM, the p-xylene dimethyl ether-linked aromatic rings inherent from

DEU-EP molecule tends to transforms to the p-xylene methane-linked aromatic structure that will promote charring of the epoxy matrix at a high temperature, therefore reducing liberation of gaseous fuels [50]. The much higher char yield of DEU-EP/DDM than that of DGEBA/DDM has been confirmed by the TG analysis (Fig. 10). Less amount of gaseous combustible in the gas phase lead to a low heat release rate. Moreover, the morphology of the residues from two systems after the MMC test is quite different as shown in Fig. 11. DGEBA/DDM shows evenly distributed residue layer at the bottom of the crucible losing its ability to keep its original shape, whereas DEU-EP/DDM shows an integrated char structure with high strength. Such impact residue structure will be helpful in slowing down the combustible gases release and propagation of burning rate in other fire tests, such as horizontal burning test.

To be more illustrative, Fig. 12 also compares the images of the horizontal burning test on the cured DGEBA/DDM and DEU-EP/DDM at the different burning time. After ignition, DGEBA/DDM burns progressively, does not extinguish after 60s until burning out finally. In contrast, impressively after ignition at the same condition DEU-EP/DDM self-extinguishes at about only 10s, showing a significantly improved resistance to the fire propagation. The reason for the observed self-extinguishing phenomenon is that DEU-EP/DDM is easy to carbonize during the combustion due to its intrinsic chemical structures. With the significantly reduced heat release and decreased rate of compatible generation, the formed char layer is strong and retard the diffusion of the fuels from the decomposed epoxy matrix to combustion zone [51]. In this case, no enough fuel and heat can maintain the propagation of fire. To conclude, the MCC results and the horizontal burning test approve DEU-EP/DDM much lower flammability than DGEBA/DDM.

Fig. 12.

4. Conclusions

We have the successfully achieved a novel eugenol-based epoxy resin (DEU-EP) with the high net biobased content (70.2%) via a facile way. With 4,4'-diaminodiphenyl methane (DDM) as the curing agent, we comparatively studied the curing reaction and final properties of DEU-EP and DGEBA of similar molecule weight. DEU-EP could be well cured by DDM, showing lower curing reactivity than DGEBA. The isothermal curing reaction of DEU/EP was autocatalytic, the Kamal model could well simulate the curing reaction rate, and the corresponding activation energies for nonautocatalytic and autocatalytic reactions were 65.4 ± 2.2 kJ/mol and 58.6 ± 2.3 kJ/mol, respectively. The isoconversional analysis showed dependent upon the conversion the DEU-EP/DDM had complicated reaction

mechanisms which are affected by not only the pure chemical reaction but also diffusion process of the reactive groups at the difference curing stages.

DEU-EP/DDM exhibited the lower glass temperature (114 ^{o}C vs. 154 ^{o}C) but higher storage and loss modulus than DGEBA/DDM up to 97 ^{o}C. DEU-EP/DDM expressed higher Young's (3490 ± 60 MPa vs. 4200 ± 140 MPa) and hardness (298.6 ± 9.2 MPa vs. 319.2 ± 16.2 MPa) than DGEBA/DDM at room temperature. DEU-EP/DDM also showed a 36% increase in the creep displacement at 600 s due to the increased chain motion ability at glass state of the material. The DEU-EP/DDM was thermally stable up 270 ^{o}C exhibiting much higher char yield than DGEBA/DDM (38% vs. 18%) in N_2 at 700 ^{o}C. DEU-EP/DDM showed much lower peak of heat release rate (201 ± 7 W/g vs. 447 ± 18 W/g) and total heat release (16.3 ± 0.8 kJ/g vs. 26.6 ± 0.9 kJ/g) than DGEBA/DDM. Interestingly, DEU-EP/DDM self-extinguished in a short time (10s) but DGEBA/DDM burned out in horizontal burning test. Therefore, DEU-EP/DDM exhibited much reduced flammability compared to DGEBA/DDM.

To summarize, our study provides a facile but highly efficient strategy to develop the high-biocontented eugenol-based epoxy resin with high rigidity and low flammability, and better illustrates how eugenol building block affect the curing reaction, kinetics and mechanisms, thermal decomposition, thermomechanical mechanical performance and flammability of DEU-EP/DDM. Our work provides a good starting point of sustainable biobased epoxy resin with high biobased content, rigidity and reduced flammability, which will advance application potentials of biobased epoxy resins. Beyond other current work, there are still challenging from chemical and materials engineering point of view to explore the more effective, scalable and atom-efficient method to epoxidize double bonds of eugenol-based epoxy precursor. This method may be somewhat different from the industrially well-established methods for epoxidized soybean oils due to the different chemical environment of the double bonds inherent from eugenol molecules.

Acknowledgements

The research leading to these results has received funding from the European Union Seventh Framework Programme (FP7 2007-2013) under grant agreement PIIF-GA-2013-626682. This work is also partially funded by the European Project COST Action MP1105 "FLARETEX", and Ramón y Cajal grant (RYC-2012-10737). We would like to express our especial thanks to the expert reviewers for their professional and constructive comments on our paper.

Supporting information

^{1}H-NMR, ^{13}C-NMR spectrum and GPC profile of bisphenol A epoxy resin (DGEBA), FTIR spectra of the intermediate (DEU) and eugenol-based epoxy resin (DEU-EP), and nonisothermal DSC profiles of pure eugenol-based epoxy resin (DEU-EP).

Figure captains

Fig. 1. (a) ^{1}H-NMR spectra of DEU and DEU-EP, (b) ^{13}C-NMR spectrum and (c) GPC traces of DEU and DEU-EP (THF, 35 ^{o}C and RI Signal). The ^{1}H-NMR chemical shifts of DEU and DEU-EP agree with their molecular structures. DEU shows the double bond related chemical shifts at 3.28, 5.00, 5.02 and 5.89 ppm, whereas DEU-EP shows the epoxy ring related ^{1}H-NMR chemical shifts at 2.54, 2.80 and 3.12 ppm. The ^{13}C-NMR chemical shifts of DEU-EP agree well with its expected molecular structure, where signals at 47.1 and 52.8 ppm correspond to the carbon on the epoxy rings. GPC relative molecular weights of eugenol and DEU-EP (158 and 428) is close to their expected molecular weights of eugenol and DEU-EP (164 and 462).

Fig. 2. Nonisothermal thermographs of DEU-EP/DDM and DGEBA/DDM with the heating rate of 10K/min. DEU-EP/DDM (red line) shows the two melting processes due to DDM and DEU-EP, followed by the exothermic curing process with the peak temperature of 166 ^{o}C. DGEBA/DDM (black line) only shows a strong exothermic thermal curing process with the peak temperature of 161 ^{o}C.

Fig. 3. DSC thermographs and conversion curves of curing reaction of DEU-EP/DDM and DGEBA/DDM. Fig. 3a compares the heat flow and fractional conversion of DEU-EP/DDM and DGEBA/DDM at 140 ^{o}C with peak heat flow values of -0.6057 W/g and -0.3981 W/g, respectively. Fig. 3b displays the evolution of heat flow and conversion of DEU-EP/DDM changes with reaction time for 120, 125, 135 and 140 ^{o}C.

Fig. 4. Isothermal curing reaction rate of DEU-EP/DDM as a function of conversion. The experimental and predicated curing rate from equation (1) for the different isothermal temperatures of 120, 125, 135, and 140 ^{o}C are indicated by the full lines and the dotted lines, respectively.

Fig. 5. Arrhenius plots of logarithmic rate constant ($\ln k_1$ and $\ln k_1$) against inverse absolute temperature (1/K). Solid cycles are for the autocatalytic reaction and solid squares is for the nonautocatalytic reaction according to the Kamal

model. The red lines are obtained by fitting these data points linearly, and R_1 and R_2 are the linear correlation coefficient.

Fig. 6. Effective activation energy (E_α) as a function of fractional conversion (α) for the isothermal curing reaction at 120, 125, 135 and 140 ^oC. E_α is determined by using the isoconversional Vyazovkin method, equations (2a and 2b).

Fig. 7. Representative dynamic mechanical spectrafor storage and loss modulus and Tan Delta of the cured DGEBA/DDM and DEU-EP/DDM (1 Hz, 3 ^oC/min).

Fig. 8. Representative load–displacement curves of DGEBA/DDM and DEU-EP/DDM with maximum load of 9000 μN. The loading, unloading rate and holding time at peak load are 300 μN/s, 450 μN/s and 5 s, respectively. From the obtained unloading segment, the hardness (H) and Young's modulus (E) can be calculated. DGEBA/DDM and DEU-EP/DDM have the elastic module and hardness of 3490 ± 60 MPa, 4200 ± 140 MPa, 298.6 ± 9.2 MPa, and 319.2 ± 16.2 MPa, respectively.

Fig. 9. Typical curves of creep displacement against time for DGEBA/DDM and DEU-EP/DDM with a constant load of 9000 μN. DGEBA/DDM and DEU-EP/DDM show accumulated creep displacement (600 s) of 107.5 ± 13.7 and 146.2 ±10.4 nm, respectively.

Fig. 10. TG and DTG thermographs of cured DGEBA/DDM and DEU-EP/DDM with heating rate of 10 ^oC /min in N_2. The solid lines indicates the TG thermographs and dotted lines indicates DTG thermographs. DEGBA/DDM shows no apparent weight loss up to 320 ^oC and the char yield of 18% at 700 ^oC, and DEU-EP/DDM begins to decompose at 280 ^oC and has the char yield of 38%. DGEBA/DDM and DEU-EP/DDM and shows the maximum decomposition rate 1.736 and 0.8632 %/^oC, respectively.

Fig. 11. Heat release rate (HRR) against temperature with heating rate 1 ^oC/s registered on the microscale combustion calorimeter (MCC). The black lines indicates the DGEBA/DDM and red line indicates DEU-EP/DDM. DEU-EP/DDM shows much lower heat release rate at peak (PeakHRR) and total heat release (Total HR) than DGEBA/DDM (447 ± 18 W/g vs. 201 ± 7 W/g and 26.6 ± 0.9 kJ/g vs. 16.3 ± 0.8 kJ/g). After the MMC test, DEU-EP/DDM show an integrated char structure, whereas DGEBA/DDM show evenly distributed char structure without maintaining the original shape of sample.

Fig. 12. Images of the horizontal burning test with the burning time of 10s. The top three figures of burning of DEGBA/DDM corresponds to the starting time, 30s and 60s; bottom three figures of DEU-EP/DDM denote the starting time, 5s and 10s, respectively. DEU-EP/DDM self-extinguishes at about 10s, whereas DGEBA/DDM is still burning after 60s. Horizontal burning tests were conducted on the cured epoxy resins.

References

[1] C.A. May, Epoxy Resins Chemistry and Technology (2nd Edition). Marcel Dekker, Inc, 1988.
[2] E.M. Petrie, Epoxy Adhesive Formulations. McGraw-Hill Publishing, 2006.
[3] C. Aouf, C. Le Guernevé, S. Caillol, H. Fulcrand, Study of the O-glycidylation of natural phenolic compounds. The relationship between the phenolic structure and the reaction mechanism, Tetrahedron 69 (2013) 1345-1353.
[4] A. Campanella, C. Fontanini, M.A. Baltanás, High yield epoxidation of fatty acid methyl esters with performic acid generated in situ, Chem. Eng. J. 144 (2008) 466-475.
[5] E. Santacesaria, R. Tesser, M. Di Serio, R. Turco, V. Russo, D. Verde, A biphasic model describing soybean oil epoxidation with H2O2 in a fed-batch reactor, Chem. Eng. J. 173 (2011) 198-209.
[6] J.M. Gibson, P.S. Thomas, J.D. Thomas, J.L. Barker, S.S. Chandran, M.K. Harrup, K.M. Draths, J.W. Frost, Benzene-free synthesis of phenol, Angew. Chem. Int. Ed. 40 (2001) 1945-1948.
[7] B.M. Bell, J.R. Briggs, R.M. Campbell, S.M. Chambers, P.D. Gaarenstroom, J.G. Hippler, B.D. Hook, K. Kearns, J.M. Kenney, W.J. Kruper, D.J. Schreck, C.N. Theriault, C.P. Wolfe, Glycerin as a Renewable Feedstock for Epichlorohydrin Production. The GTE Process, CLEAN – Soil, Air, Water 36 (2008) 657-661.
[8] E. Santacesaria, R. Tesser, M. Di Serio, L. Casale, D. Verde, New Process for Producing Epichlorohydrin via Glycerol Chlorination, Ind. Eng. Chem. Res. 49 (2010) 964-970.
[9] R. Auvergne, S. Caillol, G. David, B. Boutevin, J.-P. Pascault, Biobased Thermosetting Epoxy: Present and Future, Chem. Rev. 114 (2014) 1082-1115.
[10] C. Ding, A.S. Matharu, Recent Developments on Biobased Curing Agents: A Review of Their Preparation and Use, ACS Sustainable Chem. Eng. 2 (2014) 2217-2236.
[11] M. Stemmelen, F. Pessel, V. Lapinte, S. Caillol, J.P. Habas, J.J. Robin, A Fully Biobased Epoxy Resin from Vegetable Oils: From the Synthesis of the Precursors by Thiol-ene Reaction to the Study of the Final Material, J. Polym. Sci., Part A: Polym. Chem. 49 (2011) 2434-2444.
[12] J.-M. Pin, N. Sbirrazzuoli, A. Mija, From Epoxidized Linseed Oil to Bioresin: An Overall Approach of Epoxy/Anhydride Cross-Linking, ChemSusChem 8 (2015) 1232-1243.
[13] X. Pan, P. Sengupta, D.C. Webster, High Biobased Content Epoxy-Anhydride Thermosets from Epoxidized Sucrose Esters of Fatty Acids, Biomacromolecules 12 (2011) 2416-2428.
[14] K. Huang, P. Zhang, J. Zhang, S. Li, M. Li, J. Xia, Y. Zhou, Preparation of biobased epoxies using tung oil fatty acid-derived C21 diacid and C22 triacid and study of epoxy properties, Green Chem. 15 (2013) 2466-2475.
[15] K. Huang, Z. Liu, J. Zhang, S. Li, M. Li, J. Xia, Y. Zhou, Epoxy Monomers Derived from Tung Oil Fatty Acids and Its Regulable Thermosets Cured in Two Synergistic Ways, Biomacromolecules 15 (2014) 837-843.
[16] F. Hu, J.J. La Scala, J.M. Sadler, G.R. Palmese, Synthesis and Characterization of Thermosetting Furan-Based Epoxy Systems, Macromolecules 47 (2014) 3332-3342.
[17] J. Hong, D. Radojcic, M. Ionescu, Z.S. Petrovic, E. Eastwood, Advanced materials from corn: isosorbide-based epoxy resins, Polymer Chemistry 5 (2014) 5360-5368.
[18] A. Maiorana, S. Spinella, R.A. Gross, Bio-Based Alternative to the Diglycidyl Ether of Bisphenol A with Controlled Materials Properties, Biomacromolecules 16 (2015) 1021-1031.
[19] B. Lochab, S. Shukla, I.K. Varma, Naturally occurring phenolic sources: monomers and polymers, Rsc Adv. 4 (2014) 21712-21752.

[20] L. Rojo, B. Vazquez, J. Parra, A.L. Bravo, S. Deb, J.S. Roman, From natural products to polymeric derivatives of "eugenol": A new approach for preparation of dental composites and orthopedic bone cements, Biomacromolecules 7 (2006) 2751-2761.
[21] M. Neda, K. Okinaga, M. Shibata, High-performance bio-based thermosetting resins based on bismaleimide and allyl-etherified eugenol derivatives, Mater. Chem. Phys. 148 (2014) 319-327.
[22] B.G. Harvey, C.M. Sahagun, A.J. Guenthner, T.J. Groshens, L.R. Cambrea, J.T. Reams, J.M. Mabry, A High-Performance Renewable Thermosetting Resin Derived from Eugenol, ChemSusChem 7 (2014) 1964-1969.
[23] V.V. Kireev, N.S. Bredov, Y.V. Bilichenko, K.A. Lysenko, R.S. Borisov, V.P. Chuev, Epoxy oligomers based on eugenol cyclotriphosphazene derivatives, Polym. Sci. Ser. A 50 (2008) 609-615.
[24] I.S. Sirotin, Y.V. Bilichenko, A.N. Solodukhin, V.V. Kireev, M.I. Buzin, R.S. Borisov, Eugenol derivatives of higher chlorocyclophosphazenes and related epoxy oligomers, Polym. Sci. Ser. B 55 (2013) 241-251.
[25] J. Qin, H. Liu, P. Zhang, M. Wolcott, J. Zhang, Use of eugenol and rosin as feedstocks for biobased epoxy resins and study of curing and performance properties, Polym. Int. 63 (2014) 760-765.
[26] C.L. Williams, C.-C. Chang, P. Do, N. Nikbin, S. Caratzoulas, D.G. Vlachos, R.F. Lobo, W. Fan, P.J. Dauenhauer, Cycloaddition of Biomass-Derived Furans for Catalytic Production of Renewable p-Xylene, ACS Catal. 2 (2012) 935-939.
[27] Z. Lin, M. Ierapetritou, V. Nikolakis, Aromatics from Lignocellulosic Biomass: Economic Analysis of the Production of p-Xylene from 5-Hydroxymethylfurfural, AIChE J. 59 (2013) 2079-2087.
[28] Y.-T. Cheng, Z. Wang, C.J. Gilbert, W. Fan, G.W. Huber, Production of p-Xylene from Biomass by Catalytic Fast Pyrolysis Using ZSM-5 Catalysts with Reduced Pore Openings, Angew. Chem. Int. Edit. 51 (2012) 11097-11100.
[29] http://ir.gevo.com/phoenix.zhtml?c=238618&p=irol-newsArticle&ID=1849755. (Lastly accessed on 08/09/2015).
[30] G.M. Pharr, A. Bolshakov, Understanding nanoindentation unloading curves, J. Mater. Res. 17 (2002) 2660-2671.
[31] Y. Li, O. Rios, M.R. Kessler, Thermomagnetic processing of liquid-crystalline epoxy resins and their mechanical characterization using nanoindentation, ACS Appl. Mater. Interfaces 6 (2014) 19456-19464.
[32] L. Shen, L. Wang, T. Liu, C. He, Nanoindentation and morphological studies of epoxy nanocomposites, Macromol. Mater. Eng. 291 (2006) 1358-1366.
[33] A. Paiva, N. Sheller, M.D. Foster, A.J. Crosby, K.R. Shull, Microindentation and Nanoindentation Studies of Aging in Pressure-Sensitive Adhesives, Macromolecules 34 (2001) 2269-2276.
[34] L. Xu, J.H. Fu, J.R. Schlup, In situ near-infrared spectroscopic investigation of epoxy resin-aromatic amine cure mechanisms, J. Am. Chem. Soc. 116 (1994) 2821-2826.
[35] B.A. Rozenberg, Kinetics, thermodynamics and mechanism of reactions of epoxy oligomers with amines, Adv. Polym. Sci. 75 (1986) 113-165.
[36] R.K. Musa, Thermoset characterization for moldability analysis, Polym. Eng. Sci. 14 (1974) 231-239.
[37] J. Wan, Z.-Y. Bu, C.-J. Xu, B.-G. Li, H. Fan, Preparation, curing kinetics, and properties of a novel low-volatile starlike aliphatic-polyamine curing agent for epoxy resins, Chem. Eng. J. 171 (2011) 357-367.
[38] J. Wan, C. Li, Z.-Y. Bu, C.-J. Xu, B.-G. Li, H. Fan, A comparative study of epoxy resin cured with a linear diamine and a branched polyamine, Chem. Eng. J. 188 (2012) 160-172.
[39] S. Vyazovkin, N. Sbirrazzuoli, Mechanism and kinetics of epoxy-amine cure studied by differential scanning calorimetry, Macromolecules 29 (1996) 1867-1873.
[40] S. Vyazovkin, N. Sbirrazzuoli, Isoconversional kinetic analysis of thermally stimulated processes in polymers, Macromol. Rapid Commun. 27 (2006) 1515-1532.
[41] S. Vyazovkin, A.K. Burnham, J.M. Criado, L.A. Pérez-Maqueda, C. Popescu, N. Sbirrazzuoli, ICTAC Kinetics Committee recommendations for performing kinetic computations on thermal analysis data, Thermochim. Acta 520 (2011) 1-19.
[42] M.R. Saeb, F. Najafi, E. Bakhshandeh, H.A. Khonakdar, M. Mostafaiyan, F. Simon, C. Scheffler, E. Mäder, Highly curable epoxy/MWCNTs nanocomposites: An effective approach to functionalization of carbon nanotubes, Chem. Eng. J. 259 (2015) 117-125.
[43] H. Stutz, J. Mertes, Influence of the structure on thermoset cure kinetics, J. Polym. Sci., Part A: Polym. Chem. 31 (1993) 2031-2037.
[44] J. Wan, C. Li, Z.-Y. Bu, H. Fan, B.-G. Li, Acrylonitrile-capped poly(propyleneimine) dendrimer curing agent for epoxy resins: Model-free isoconversional curing kinetics, thermal decomposition and mechanical properties, Mater. Chem. Phys. 138 (2013) 303-312.
[45] S. Cukierman, J.-L. Halary, L. Monnerie, Dynamic mechanical response of model epoxy networks in the glassy state, Polym. Eng. Sci. 31 (1991) 1476-1482.

[46] M. Aldridge, A. Wineman, A. Waas, J. Kieffer, In Situ Analysis of the Relationship between Cure Kinetics and the Mechanical Modulus of an Epoxy Resin, Macromolecules 47 (2014) 8368-8376.
[47] M.E. Dokukin, I. Sokolov, On the Measurements of Rigidity Modulus of Soft Materials in Nanoindentation Experiments at Small Depth, Macromolecules 45 (2012) 4277-4288.
[48] F. Haw James, P. Schultz Tor, Carbon-13 CP/MAS NMR and FT-IR Study of Low-Temperature Lignin Pyrolysis, Holzforschung 39 (1985) 289.
[49] J. Wan, S. Wang, C. Li, D. Zhou, J. Chen, Z. Liu, L. Yu, H. Fan, B.-G. Li, Effect of molecular weight and molecular weight distribution on cure reaction of novolac with hexamethylenetetramine and properties of related composites, Thermochim. Acta 530 (2012) 32-41.
[50] X. Wang, W. Xing, X. Feng, B. Yu, H. Lu, L. Song, Y. Hu, The effect of metal oxide decorated graphene hybrids on the improved thermal stability and the reduced smoke toxicity in epoxy resins, Chem. Eng. J. 250 (2014) 214-221.
[51] F. Laoutid, L. Bonnaud, M. Alexandre, J.M. Lopez-Cuesta, P. Dubois, New prospects in flame retardant polymer materials: From fundamentals to nanocomposites, Mat. Sci. Eng. R 63 (2009) 100-125.